

# Comparison of SNOMAN's Cherenkov Light Distribution to a Single-Scattering Model

C.J. Jillings and T.J. Radcliffe  
Queen's University  
August 1996

## 1 Introduction

The Cherenkov light distribution from an electron in water is important, especially for pattern recognition. The processes involved are sufficiently complicated that exact calculation is impossible in a code like SNOMAN. How to handle the problem is complicated by at least two things. Firstly, SNOMAN uses EGS4 to do electron transport. EGS uses Moliere multiple-scattering theory. While this theory is an excellent approximation in describing the electron track on scales of 10 microns, it does not attempt to analyse tracks on smaller scales because fundamental assumptions of the theory do not hold. However, these smaller scales do affect the Cherenkov light distribution.

Secondly, the light is not really emitted by the electron. It is emitted by the  $10^{15}$  or so water molecules nearby in some coherent way. Therefore, to say the photon was emitted at some specific point along the electron track is probably meaningless.

## 2 SNOMAN's Algorithm

SNOMAN uses a two-dimensional interpolation technique to deal with the large electron steps created by EGS. See figure 1 for an example. Note that the interpolated electron path always lies in the plane defined by the direction at the start of the step and the direction at the start of the next step.

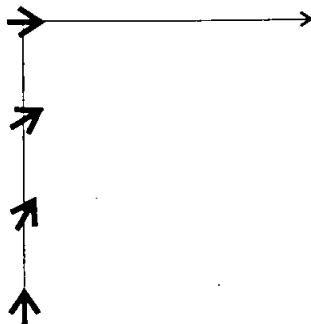


Figure 1: Two hypothetical steps from EGS are shown in thin lines. The first is straight up; the second, directed right. The interpolated electron direction is shown at four points along the first step. Note that all directions are in the plane of the paper. The angle between the two steps has been exaggerated for clarity.

### 3 A Procedure to test SNOMAN's algorithms

The goal of this work is to put an electron trajectory through two Cherenkov light calculations: SNOMAN's and a more exact calculation due to Dedrick. The results of the two calculations are then compared. R. Komar has written an excellent report describing Dedrick's work on Cherenkov light. In it, a formula is written to *coherently* sum the light output for a track composed of many straight line segments. I use results from this report extensively in what follows.

Our four-step procedure is as follows:

#### 3.1 Step 1

Create an electron path using the Mott cross-section formula with a small angle cutoff. This path is "single-scattered". That is to say, the length of a segment of the path is the distance between two individual scatters. This length varied statistically; it had a mean of 3.3 microns at 5 MeV. The cutoff was applied to disallow any scatters with an angle below 1 degree. This is legitimate because bends of less than one degree in short tracks do not

significantly affect coherence. The energy loss along the track was assumed to be a constant 2.2 MeV/cm.

### 3.2 Step 2

Calculate the Cherenkov light output using Dedrick's formula. (This takes hours on a moderately fast computer.) One calculation results in a the output as a function of  $\theta$  and  $\phi$  on a grid of, say, 180 by 360. Because this grid is finer than the resolution of SNO's "eyeball", we then averaged over adjacent bins to get a distribution. The distribution was then multiplied by the phase space factor,  $\sin \theta$ , to obtain a yield as a function of  $\theta$  and  $\phi$ . This distribution is for a particular wavelength because Dedrick's formula are not averaged over wavelength. We chose a wavelength of 400 nm in air. Dedrick's formula can be integrated over  $\theta$  and  $\phi$  to obtain the total yield. That is not done here. Instead the two-dimensional distribution was normalized to unit volume.

### 3.3 Step 3

"Egsify" the single-scattered path. If we are to compare justly, we need the same electron path for both Dedrick's formula and SNOMAN. Since a single-scattered path is used here in Dedrick's formula and SNOMAN uses a multiple-scattered path, we needed to create a multiple-scattered path from the single-scattered path.

The number of single scatters grouped together in a larger step is determined by energy loss. The step length in EGS is determined by an energy loss parameter, ESTEPE. SNOMAN "out of the box" has ESTEPE set to 3 percent. Therefore, we grouped the single steps such that the resultant step had an energy loss of 3% over the length of the step. That is to say, if the energy was 5.000 MeV at the start of the step, there would be just enough single scatters included in the step that the energy at the end would be 4.985 MeV.

What we are interested in is electron direction, not position. Therefore, the "egsified" path was not a series of vertices, but rather a series of directions. The directions were the tangents to the single-scattered path at the positions determined by an energy loss of ESTEPE. Also noted with the directions were the straight-line lengths between the start and end of the steps. This is necessary because light output is proportional to length.

### 3.4 Step 4

The final step is to apply the SNOMAN algorithm to the path created in step 3. Because the SNOMAN algorithm is statistical, and because we are interested here in the distribution of Cherenkov light rather than the total amount, we had the SNOMAN algorithm create a huge number of photons to ensure we were not affected significantly by statistical variations. The output of this step is a two-dimensional histogram ( $\theta$  and  $\phi$ ). The histogram was normalized and then be compared with the calculation in step two.

## 4 Results

In this section, we present results for some paths.

### 4.1 Path 1

Figure 2 shows the  $x$ - $z$ ,  $y$ - $z$  and  $E$ - $z$  projections of the single-scattered path. The electron directions were taken at the squares to create the EGS-equivalent path. Figure 4 shows the output of the calculation using Dedrick's formula (step 2). The histogram has been normalized to unit volume. Figure 3 shows the SNOMAN result (step four) also normalized to unit volume. Figure 5 shows the SNOMAN result minus the result from Dedrick's formula.

The path starts and ends on the  $z$ -axis. This is not coincidence. The single-scattered path created initially wandered randomly. That path was then rigidly rotated to bring the final point onto the  $z$ -axis. Because an approximate azimuthal symmetry has been forced on the path, the SNOMAN and Dedrick results were integrated over  $\phi$  to obtain a  $\theta$  projection. This is not a rigorous way of comparing the distributions — the point of this paper is that the results are two dimensional — but they are in clear agreement.

Figure 6 shows these projections.

### 4.2 Path 2

Figure 7 shows the  $x$ - $z$ ,  $y$ - $z$ , and  $E$ - $z$  projections of the single-scattered and path. The squares mark the points at which the electron directions were taken to create the "sc egs-equivalent" path. Figure 9 shows the output of the calculation using Dedrick's formula (step 2). The histogram has been

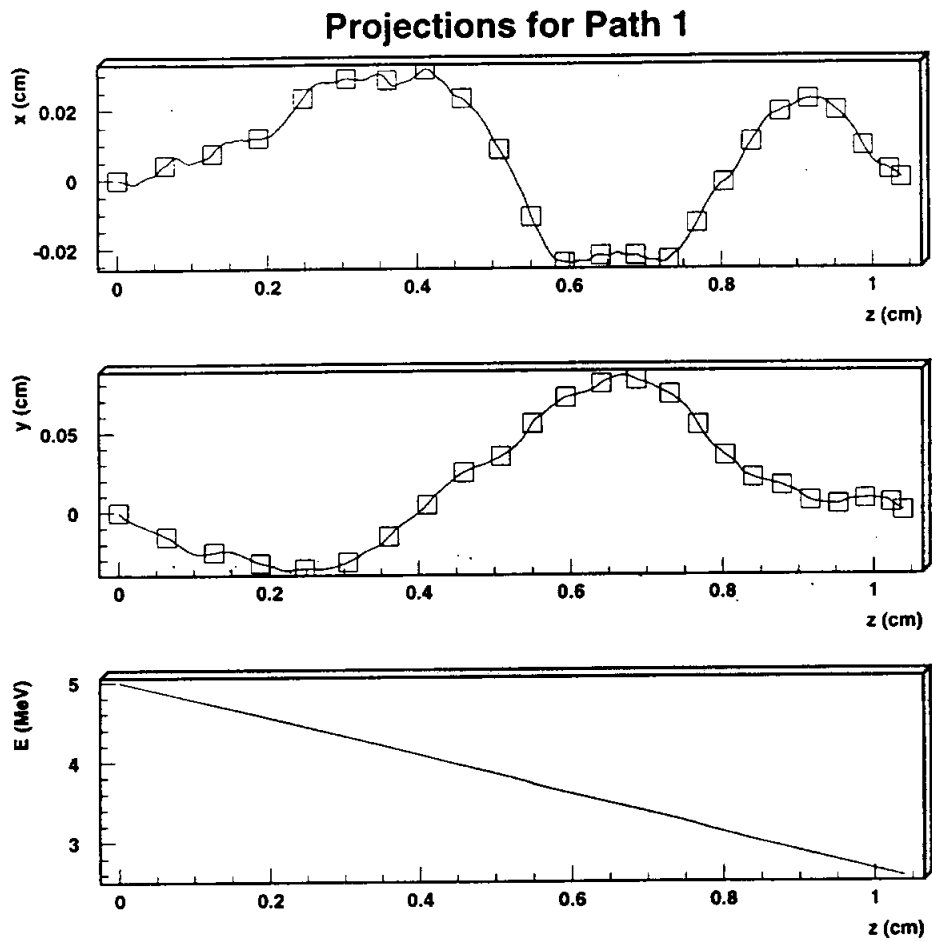


Figure 2: The  $xz$  and  $yz$  projections of a path for single scatters plotted positions at which the tangents were taken to find the EGS-equivalent path. The bottom plot shows electron energy in MeV.

### Snoman: Path 1

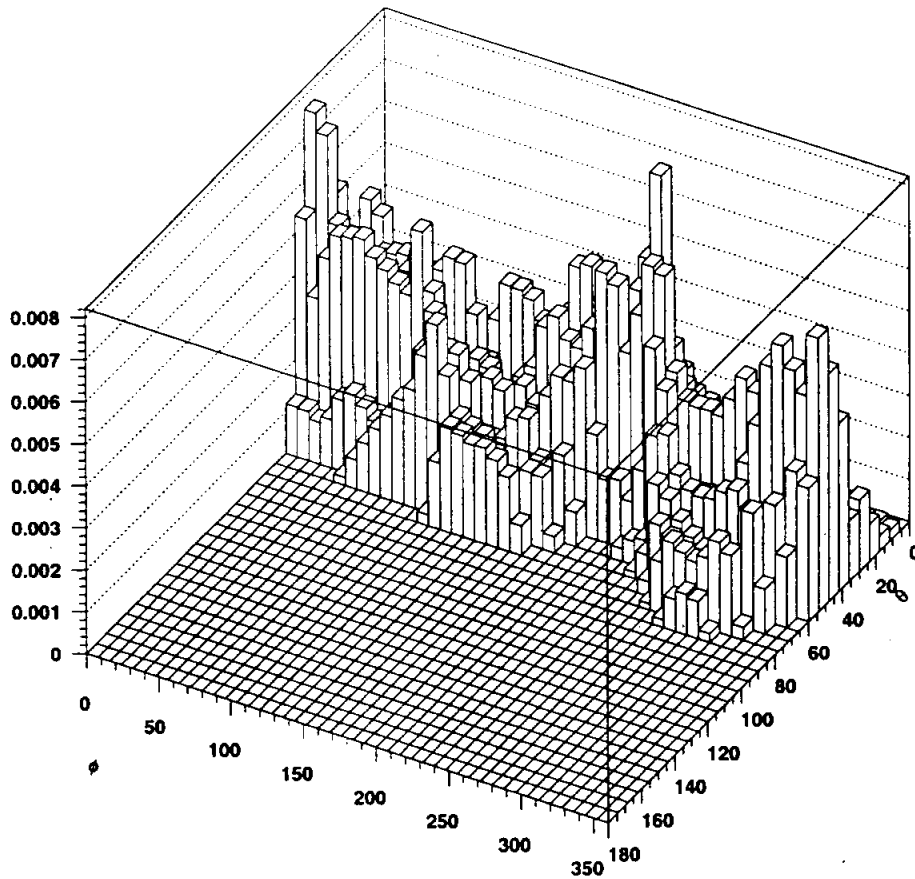


Figure 3: The output for path 1 using the SNOMAN algorithm. The axis labelled 0 to 180 is  $\theta$ ; the axis labeled 0 to 360 is  $\phi$ .

### Dedrick: Path 1

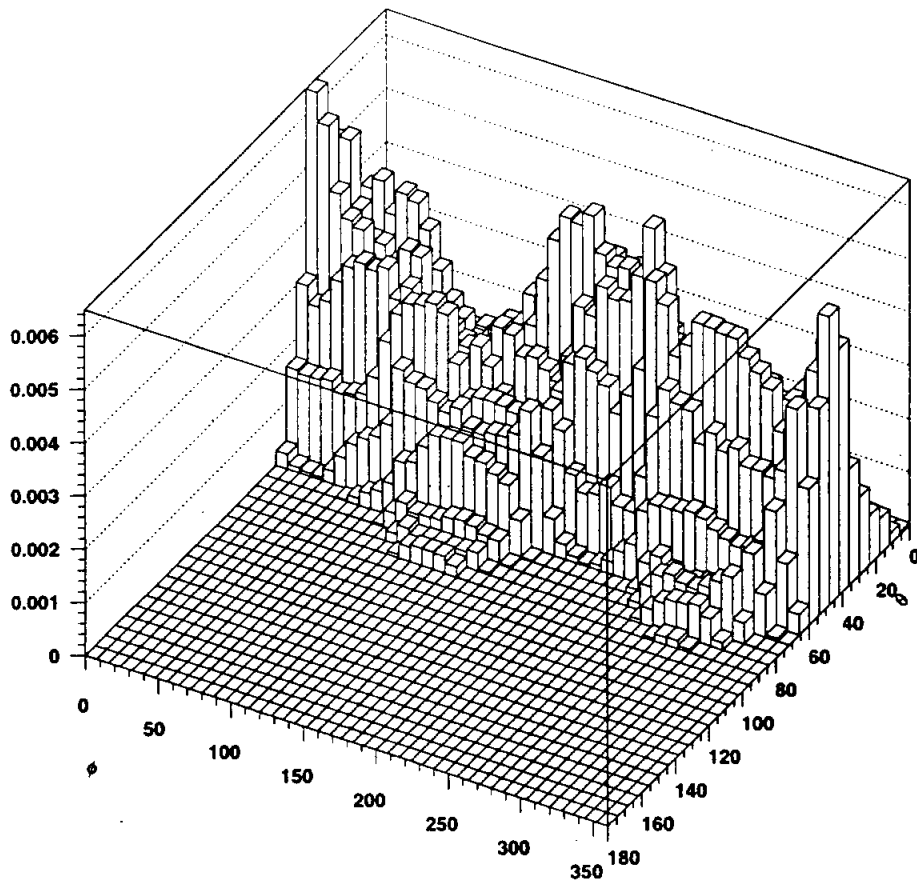


Figure 4: The output of the calculation using Dedrick's formula.

### Snoman - Dedrick: Path 1

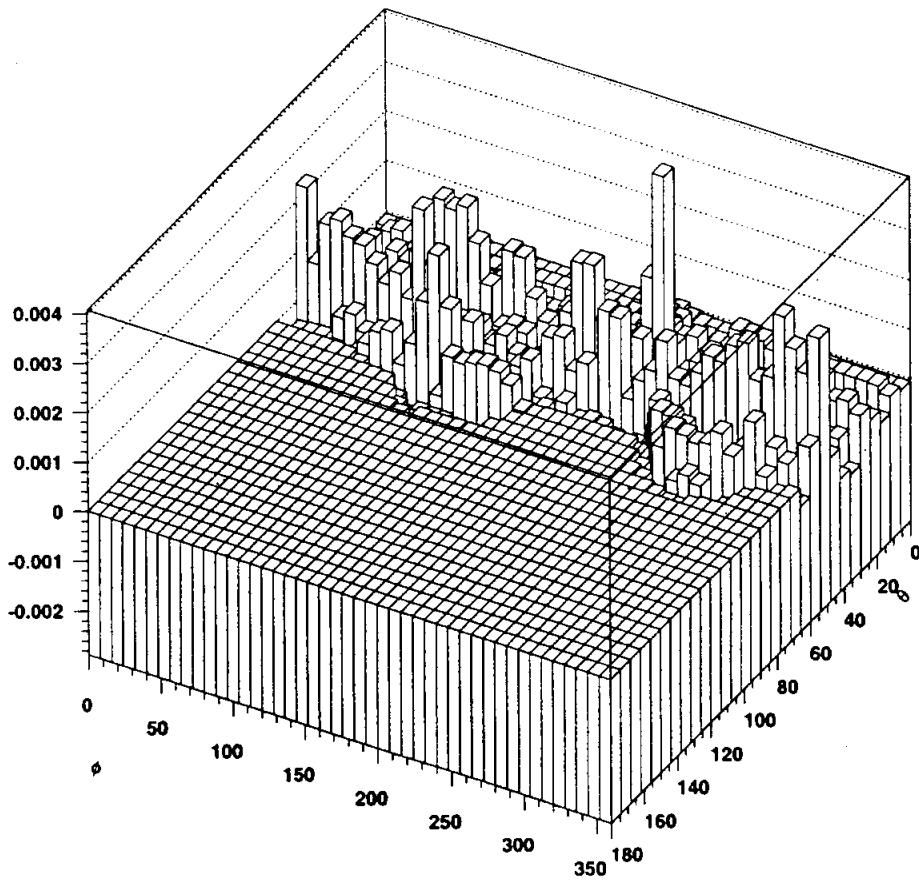


Figure 5: The difference between the SNOMAN algorithm and the result of Dedrick's formula.

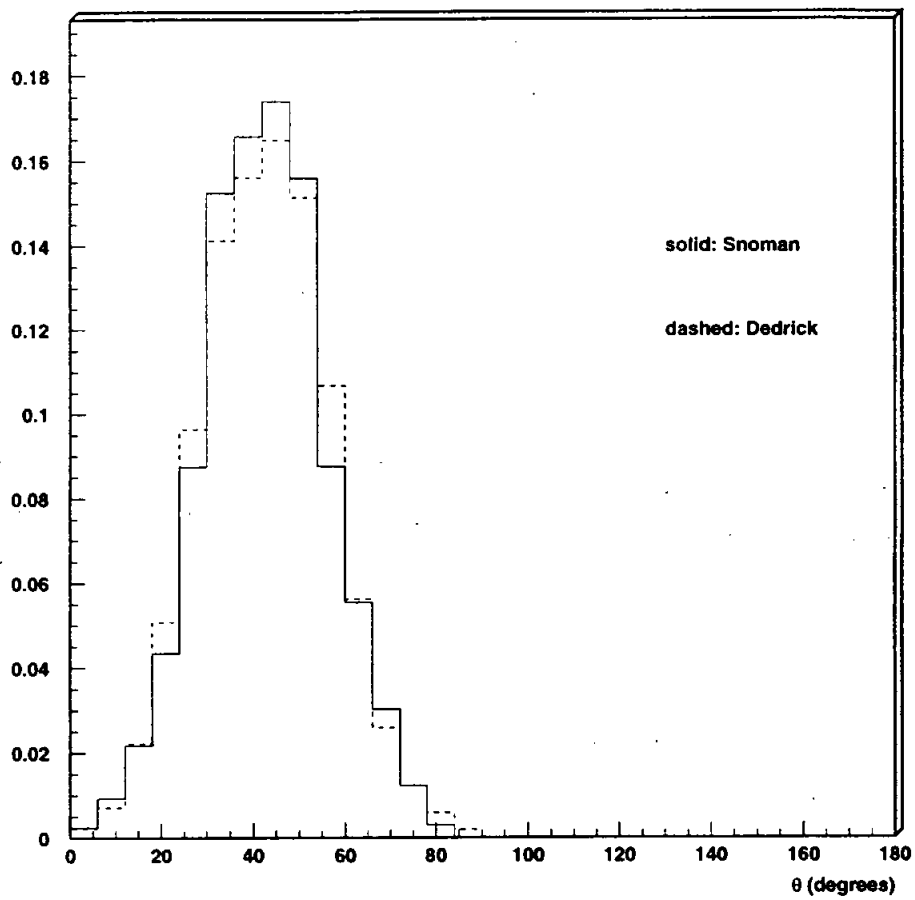


Figure 6: The projections onto  $\theta$  for path 1.

normalized to unit volume. Figure 8 shows the SNOMAN result (step four) also normalized to unit volume. Figure 10 shows the SNOMAN result minus the result from DEDRICK's formula.

### 4.3 Path 3

Figure 11 shows the  $xz$  and  $yz$  projections of the single-scattered path. The squares mark the points at which tangents were taken to create the EGS-equivalent path. Figure 13 shows the output of the calculation using DEDRICK's formula (step 2). The histogram has been normalized to unit volume. Figure 12 shows the SNOMAN result (step four) also normalized to unit volume. Figure 14 shows the SNOMAN result minus the result from DEDRICK's formula.

## 5 Discussion

The results of our calculation show that the distribution of Cherenkov light as calculated by the SNOMAN algorithm is an underestimate of the width. This discrepancy is largest at low energy. The reason for this is at least in part due to the interpolation technique. Because the interpolation is in only two dimensions of three-dimensional space, it must be at least slightly inaccurate.

Put another way, the SNOMAN algorithm forces the interpolated electron track to lie in the plane defined by the direction at the start of the step and at the end of the step. There is no way in the SNOMAN calculation to include the possibility that the electron travelled in, say, a helical path. Figure 1 gives an example of this to illustrate the point.

There are some implications for pattern recognition. At higher energies the distributions compared here are probably similar enough that to indicate SNOMAN is useful, but perhaps only as a guide to what may work. At low energies the differences may well be large enough to "trick" the algorithms into searching for artifacts. Extreme care must be taken before using SNOMAN to study, for example, the differences between Thallium and Bismuth hit patterns.

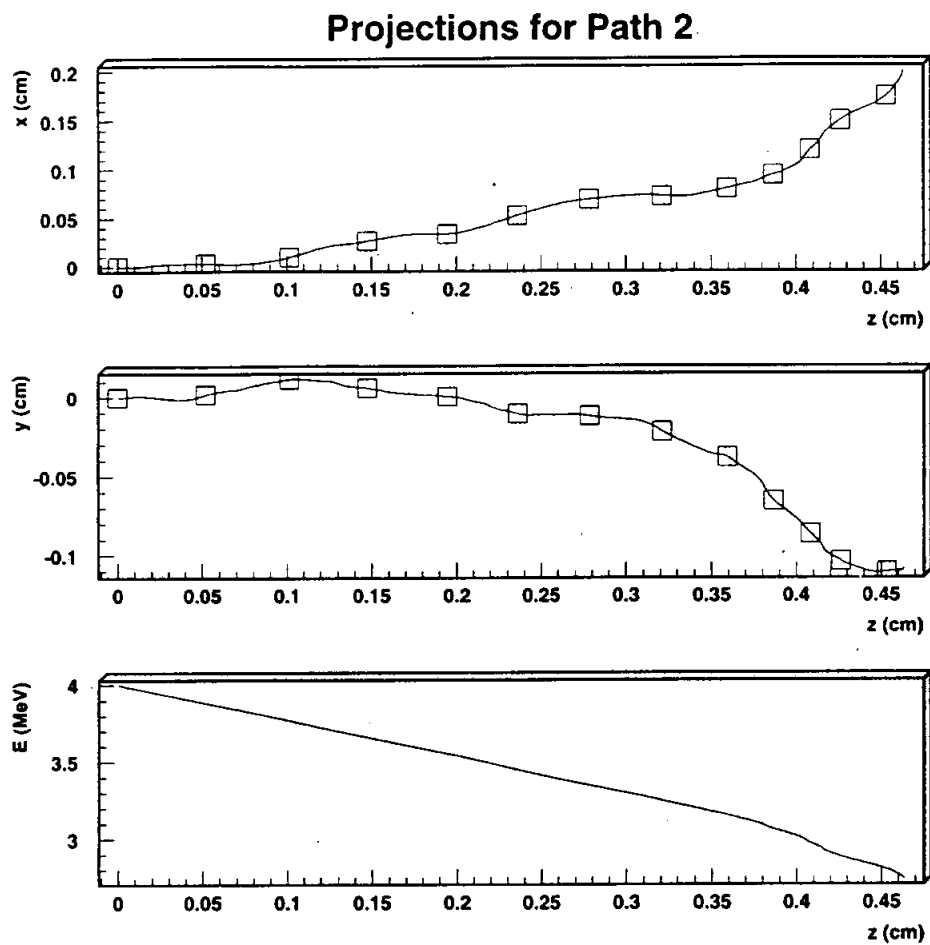


Figure 7: The  $xz$  and  $yz$  projections of a path for single scatters. The squares mark the points at which tangents were taken to create the EGS-equivalent path. The bottom plot shows electron energy in MeV.

### Snoman: Path 2

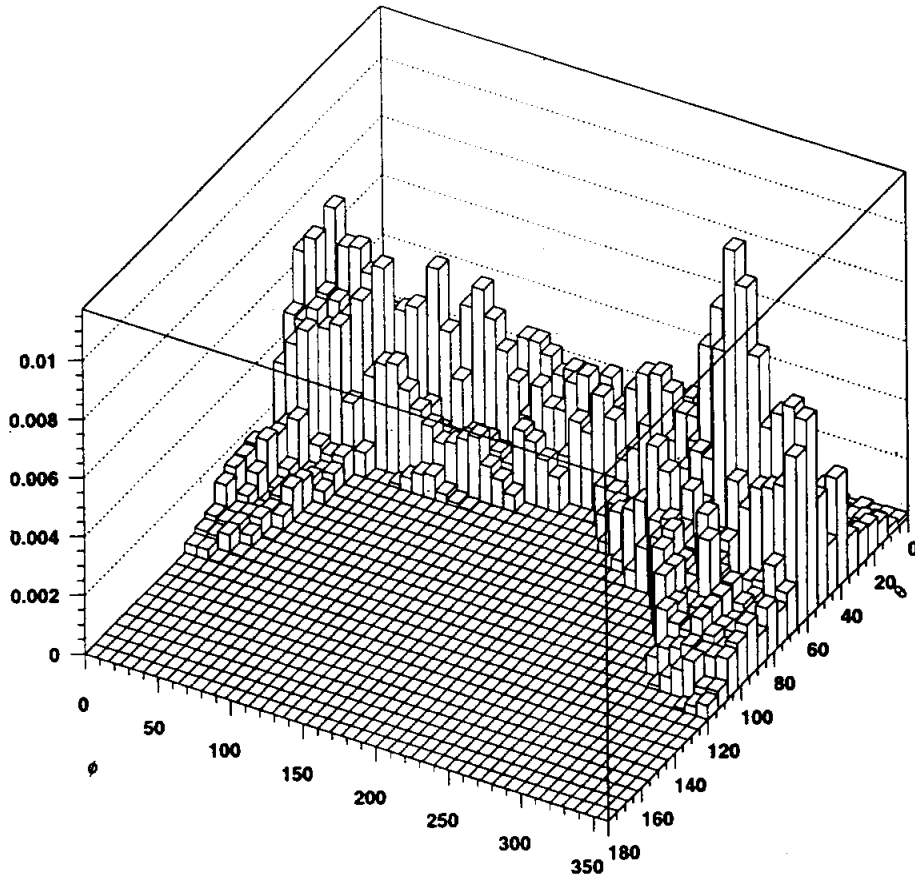


Figure 8: The output for path 2 using the SNOMAN algorithm.

### Dedrick: Path 2

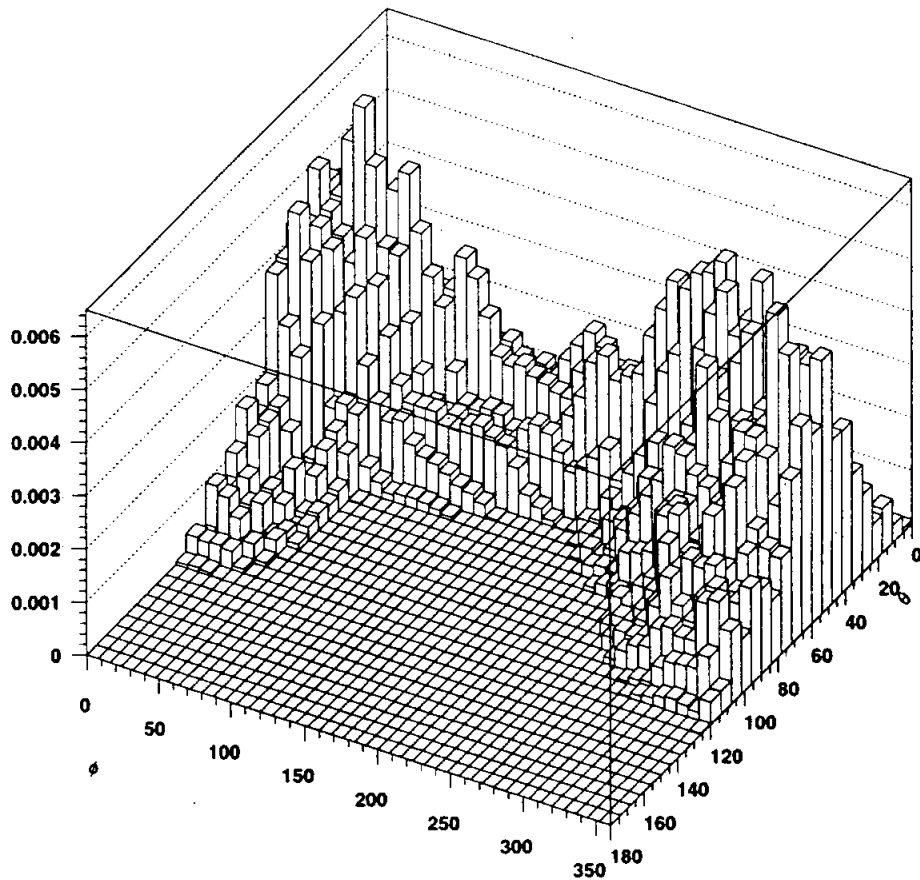


Figure 9: The output of the calculation using Dedrick's formula.

### Snoman - Dedrick: Path 2

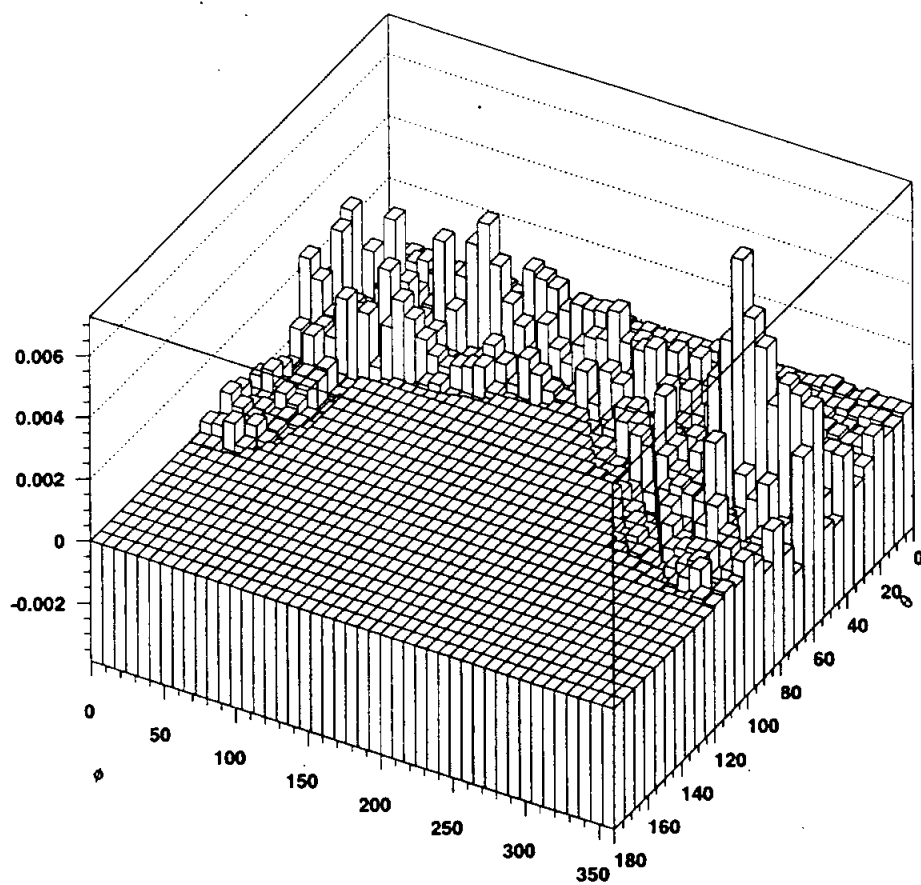


Figure 10: The difference between the SNOMAN algorithm and the result of Dedrick's formula.

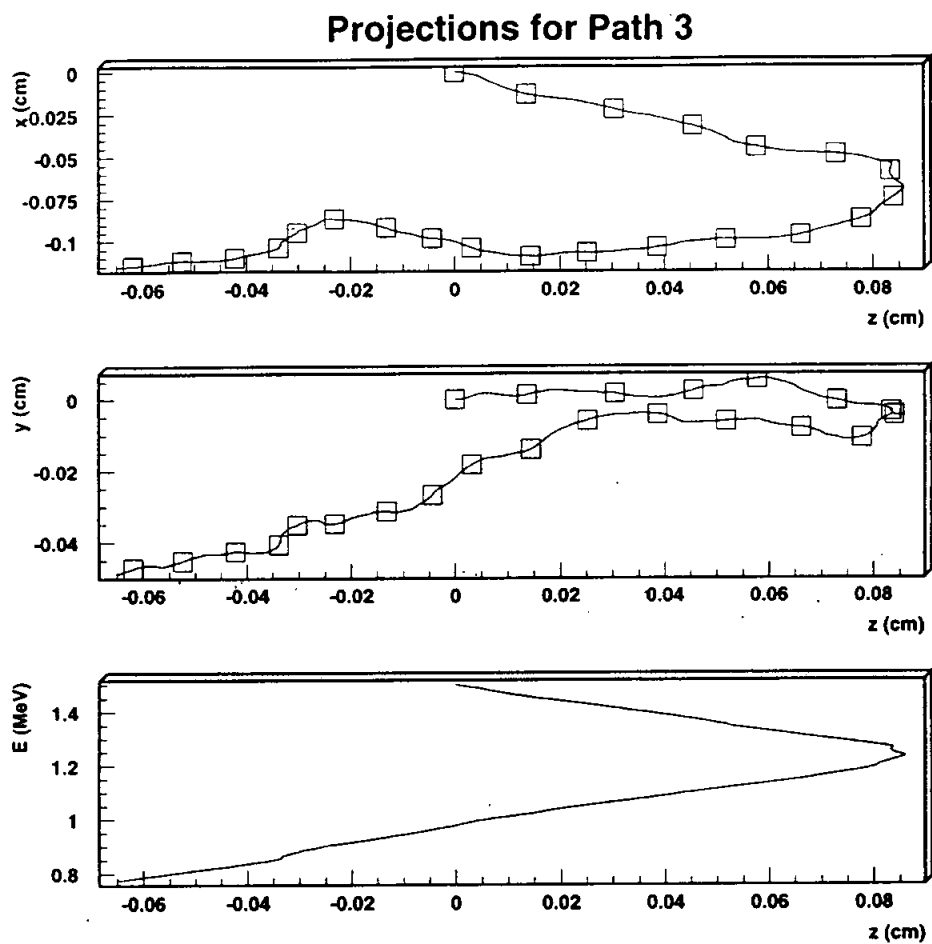


Figure 11: The  $xz$  and  $yz$  projections of a path for single scatters. The squares mark the points at which the tangents were taken to find the EQS-equivalent path. The bottom plot shows electron energy in MeV.

### Snoman: Path 3

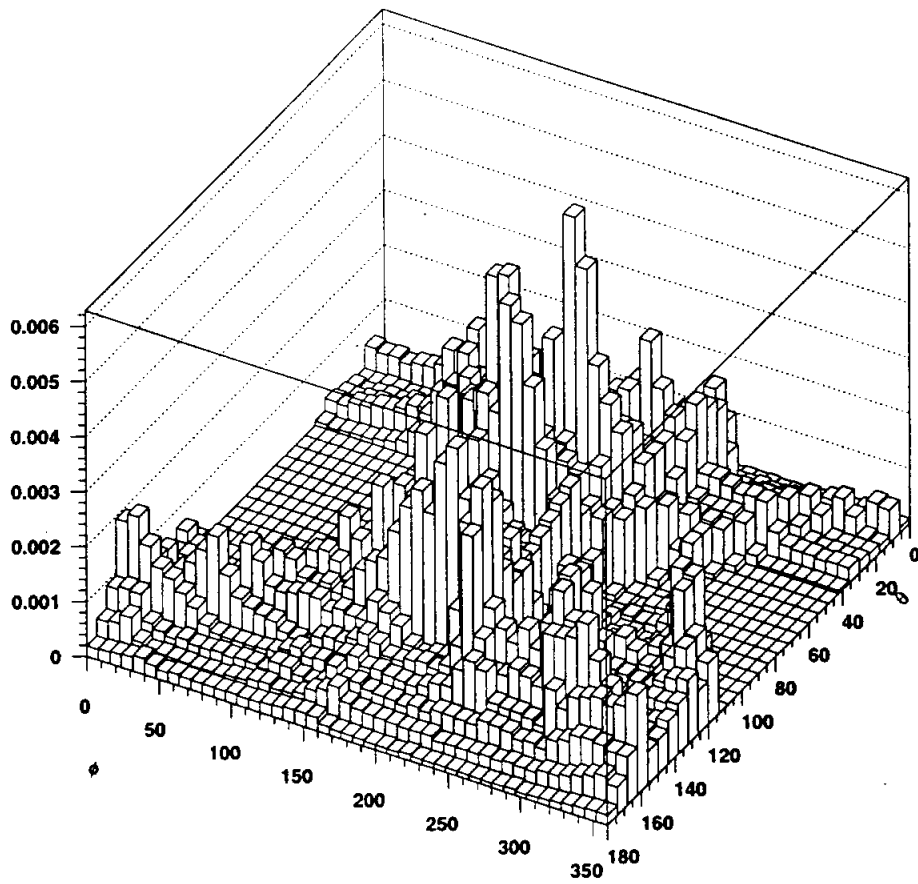


Figure 12: The output for path 3 using the SNOMAN algorithm.

### Dedrick: Path 3

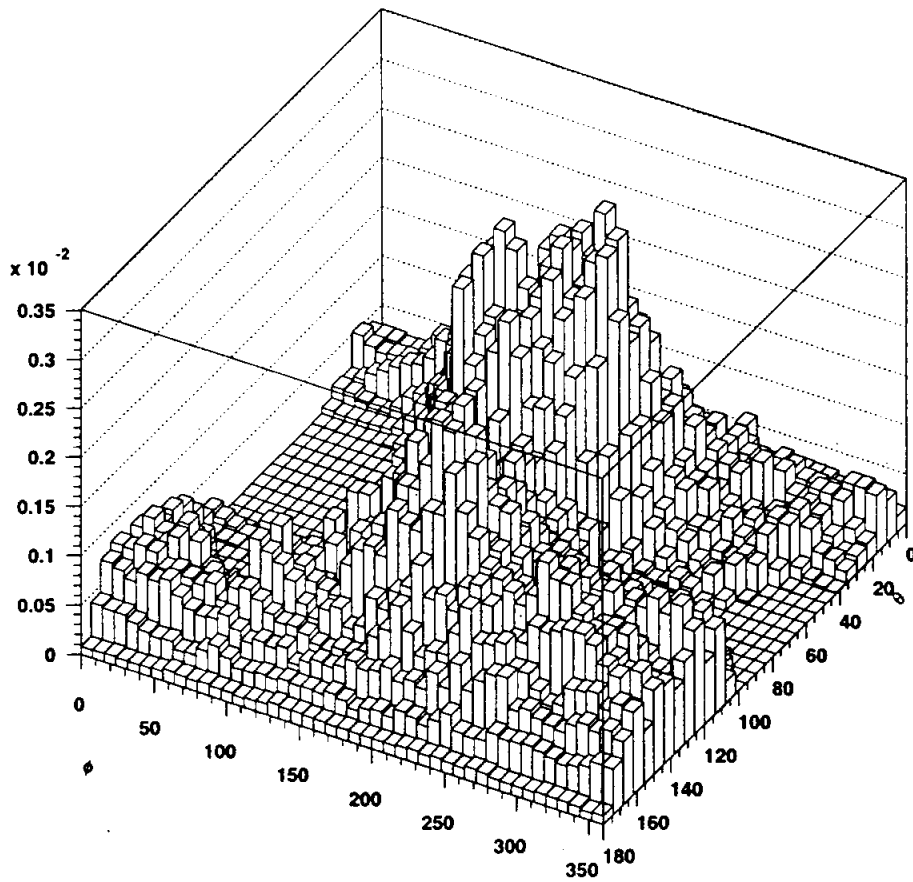


Figure 13: The output of the calculation using Dedrick's formula.

### Snoman - Dedrick: Path 3

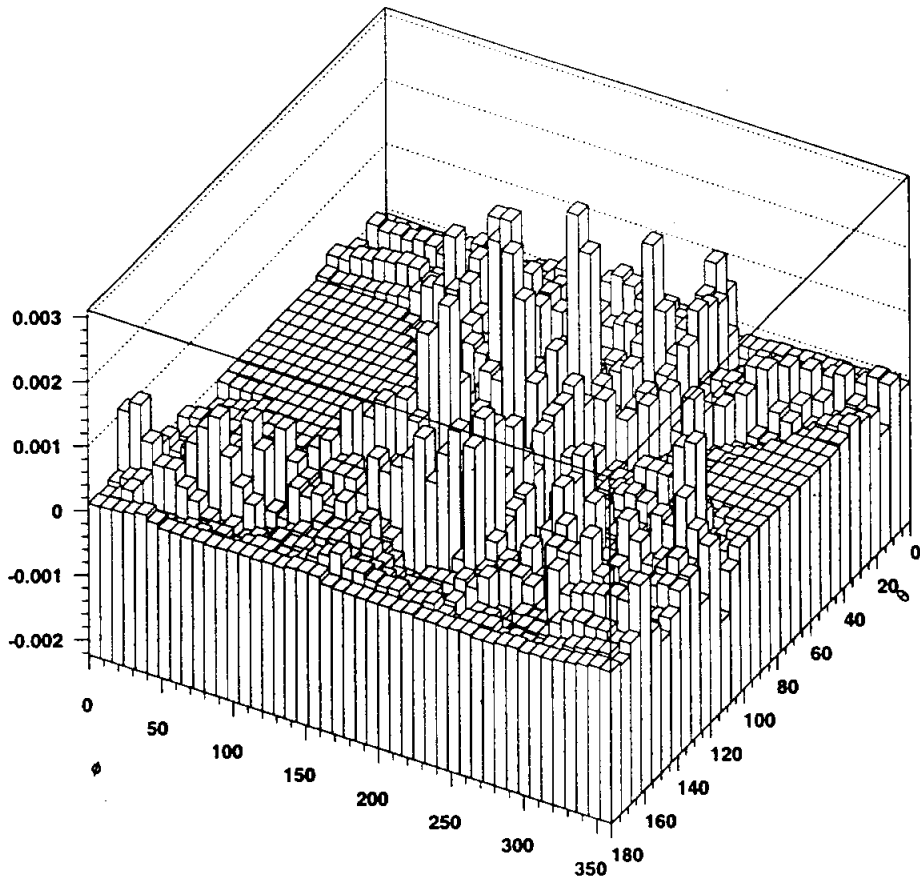


Figure 14: The difference between the SNOMAN algorithm and the result of Dedrick's formula.

## 6 Conclusion

The algorithm currently being employed in SNOMAN is almost certainly acceptable for most uses. However, users should hesitate to trust the algorithm to look for fine effects at low energies. We would discourage trusting the current SNOMAN algorithm to search for pattern differences between  $^{214}\text{Bi}$  and  $^{208}\text{Thalium}$ .

The next step in the analysis of Cherenkov light is to study the effects of a bending path on the frequency distribution of the Cherenkov light.

## 7 Acknowledgements

We would like to thank Mike Bowler for pointing out an error in our original "egsification" technique. His suggestion for an improved technique was appreciated (and used).

Thanks to Aksel Hallin, Peter Skensved, Art McDonald, Mike Lay, and Mike Bowler for valuable discussions.

Thanks to Rob Komar for summarizing Dedrick's work nicely in **Effects of Electron Scattering on Cherenkov Light Output** (SNO-STR-95-67). That report is the source of formulae used in the report for the coherent sum. If you downloaded the gzipped tar file for this paper, you will find komar.tex there. Otherwise, the latex file is on the restricted sno web server at Queen's. Email Richard Ford, ford@mips2.phy.queensu.ca, if you do not yet have access.